

RESEARCH ARTICLE

The allometric scaling of oxygen supply and demand in the California horn shark, *Heterodontus francisci*

Tanya S. Prinzing¹, Jennifer S. Bigman^{1,2}, Zachary R. Skelton^{3,4}, Nicholas K. Dulvy¹ and Nicholas C. Wegner^{4,5,*}

ABSTRACT

The gill surface area of aquatic ectotherms is thought to be closely linked to the ontogenetic scaling of metabolic rate, a relationship that is often used to explain and predict ecological patterns across species. However, there are surprisingly few within-species tests of whether metabolic rate and gill area scale similarly. We examined the relationship between oxygen supply (gill area) and demand (metabolic rate) by making paired estimates of gill area with resting and maximum metabolic rates across ontogeny in the relatively inactive California horn shark, *Heterodontus francisci*. We found that the allometric slope of resting metabolic rate was 0.966 ± 0.058 ($\pm 95\%$ CI), whereas that of maximum metabolic rate was somewhat steeper (1.073 ± 0.040). We also discovered that the scaling of gill area shifted with ontogeny: the allometric slope of gill area was shallower in individuals < 0.203 kg in body mass (0.564 ± 0.261), but increased to 1.012 ± 0.113 later in life. This appears to reflect changes in demand for gill-oxygen uptake during egg case development and immediately post hatch, whereas for most of ontogeny, gill area scales in between that of resting and maximum metabolic rate. These relationships differ from predictions of the gill oxygen limitation theory, which argues that the allometric scaling of gill area constrains metabolic processes. Thus, for the California horn shark, metabolic rate does not appear limited by theoretical surface-area-to-volume ratio constraints of gill area. These results highlight the importance of data from paired and size-matched individuals when comparing physiological scaling relationships.

KEY WORDS: Aerobic scope, Aquatic respirometry, Elasmobranch, Gill oxygen limitation, Gill surface area, Metabolic rate

INTRODUCTION

Metabolic rate underlies biological processes as it represents the allocation of energy to organismal survival, growth and reproduction (Brown et al., 2004; Sibly et al., 2012). Thus, the


change in or scaling of an organism's metabolic rate with body mass and the physiological underpinnings of this relationship are of great interest in the fields of physiology and ecology, and are deeply intertwined with organismal behavior and life history (Brown et al., 2004; Glazier, 2005; White et al., 2022). The rate of oxygen consumption (M_{O_2}), used as a proxy for metabolic rate, follows a non-linear, power-law relationship with body mass in which $M_{O_2} = aM^b$, where a is the species-specific coefficient or intercept, M is body mass and b is the scaling exponent or allometric slope of the relationship. Recently, the allometric slope of metabolic rate and other physiological allometries has garnered particular interest as it has been used to link fish metabolic physiology to changes in fish body size and geographic distributions associated with climate warming (e.g. gill oxygen limitation theory, metabolic index, aerobic growth index; Cheung et al., 2013; Clark et al., 2013; Deutsch et al., 2015; Clarke et al., 2021; Pauly, 2021). As species-specific metabolic rate estimates continue to be compiled and compared, it has become clear that the intraspecific (ontogenetic) allometric slope of metabolic rate varies widely among species (Glazier, 2005, 2010; White et al., 2006; Norin and Gamperl, 2017). In fishes, the mean ontogenetic allometric slope of metabolic rate appears to be around $b = 0.89$ (Jerde et al., 2019), although this value appears to differ among fish groups with different activity levels and habitats (Killen et al., 2010).

Historically, most studies on organismal metabolism have focused on resting metabolic rates (RMRs). However, more recent work has recognized the importance of determining an organism's maximum metabolic rate (MMR), which often scales with a steeper (higher) allometric slope than that of RMR and body mass (Brett and Glass, 1973; Killen et al., 2007; Glazier, 2009; Auer et al., 2017). Examining the allometry of both RMR and MMR provides insight into a species' aerobic scope, or capacity for energy expenditure above rest, and how that may change as an organism increases in size. Importantly, for water-breathing ectotherms such as fishes, aerobic scope is thought to be an indicator of an organism's ability to respond to environmental extremes, with species having higher aerobic scopes (and, thus, having higher oxygen requirements above baseline) generally being more sensitive to changes in temperature and dissolved oxygen level (Pörtner and Knust, 2007; Killen et al., 2016; Deutsch et al., 2015, 2020).

In most fishes, oxygen uptake to fuel metabolism occurs primarily at the gills. Thus, gill surface area follows a power-law relationship with body mass (Hughes, 1984; Palzenberger and Pohla, 1992; Nilsson and Östlund-Nilsson, 2008) that largely mirrors that of metabolic rate (De Jager and Dekkers, 1975; Hughes, 1972, 1982). Theoretically, gill surface area should be large enough to supply a fish with sufficient oxygen in order to allow the animal to carry out activities in excess of RMR, such as those surrounding survival, growth and reproduction (Hughes, 1984; Wegner, 2016). Thus, in most cases, the allometric slope for gill surface area should

¹Earth to Ocean Research Group, Department of Biological Sciences, Simon Fraser University, Burnaby, BC, Canada, V5A 1S6. ²Alaska Fisheries Science Center, National Marine Fisheries Service, National Oceanic and Atmospheric Administration, Seattle, WA 98115, USA. ³Ocean Associates Inc., under contract to Fisheries Resources Division, Southwest Fisheries Science Center, National Marine Fisheries Service, National Oceanic and Atmospheric Administration, La Jolla, CA 92037, USA. ⁴Scripps Institution of Oceanography, University of California San Diego, La Jolla, CA 92093, USA. ⁵Fisheries Resources Division, Southwest Fisheries Science Center, National Marine Fisheries Service, National Oceanic and Atmospheric Administration, La Jolla, CA 92037, USA.

*Author for correspondence (nick.wegner@noaa.gov)

 T.S.P., 0000-0001-5143-4325; J.S.B., 0000-0001-8070-3061; Z.R.S., 0000-0003-2422-9240; N.K.D., 0000-0002-4295-9725; N.C.W., 0000-0002-8447-1488

This is an Open Access article distributed under the terms of the Creative Commons Attribution License (<https://creativecommons.org/licenses/by/4.0>), which permits unrestricted use, distribution and reproduction in any medium provided that the original work is properly attributed.

be closer to that of MMR and body mass, as MMR would incorporate energetically expensive activities such as foraging and escaping predators (Bishop, 1999; Glazier, 2005; Hughes, 1984). However, most of the support for this idea comes from work on relatively active tuna and salmonid species, where RMR, MMR and gill surface area were each estimated in separate animals and studies (Muir and Hughes, 1969; Graham and Laurs, 1982; Hughes, 1984). In contrast, other studies have shown that gill area can scale in between that of MMR and RMR or even closer to RMR (Luo et al., 2020; Somo et al., 2023).

Understanding the intricacies of how the scaling of gill surface area, RMR and MMR relate has become more critical in light of changes in organismal oxygen demands associated with climate warming and ocean deoxygenation (Lefevre et al., 2021). Indeed, the supply of oxygen delivered to the tissues appears tightly coupled to temperature performance curves in ectothermic animals and may ultimately limit MMR and hence aerobic scope at higher temperatures (Pörtner and Knust, 2007; Pörtner and Farrell, 2008; Rubalcaba et al., 2020). Although the acquisition of environmental oxygen at the gills represents only the first step in the ‘oxygen cascade’ as oxygen is transferred from the environment through the blood and into the tissues (where it is ultimately utilized), the gill has received renewed attention owing to the gill oxygen limitation theory (GOLT). The GOLT focuses on this first step and argues that oxygen uptake at the gills may ultimately limit metabolism and the energy available for growth and other life-sustaining processes (Pauly, 2010, 2021; Pauly and Cheung, 2017). This theory has been used to predict ecological patterns and processes, particularly with regard to how species will respond to a changing climate. For example, Cheung et al. (2013) used this framework to predict that fish maximum body sizes will decline by approximately 7–12% from 2000 to 2050 because of increased constraints of oxygen acquisition at the gills under warmer temperatures.

The GOLT centers on the scaling of relative oxygen supply, or oxygen obtained at the gill surface and used for metabolism. Specifically, the GOLT argues that a two-dimensional gill surface area cannot increase at the same rate as the three-dimensional body mass it must supply with oxygen and, in turn, this mismatch limits metabolism and dependent processes as an organism grows (Pauly, 2010, 2021). This supposition results in two testable predictions associated with the scaling of gill surface area and metabolic rate. First, the GOLT argues that gill surface area cannot scale with body mass with an allometric slope at or above $b=1.0$ because of geometric limitations on the scaling of surface areas (e.g. geometric isometry would predict a surface area to volume increase of $b=0.67$, and although the GOLT recognizes that gill surface area can scale higher than 0.67, it argues it cannot scale with an allometric slope of $b \geq 1.0$; Pauly, 2010, 2021). A second way this theory can be viewed is that gill surface area would scale with a lower allometric slope than metabolic rate (i.e. the ratio of gill surface area to metabolic rate should decrease with size; Scheuffele et al., 2021).

The GOLT perspective that gill surface area limits metabolic rate is in direct contradiction to the widely accepted physiological view that gill surface area is adapted to match metabolic demand over a range of body sizes (Lefevre et al., 2017, 2018). Although gills are indeed a surface, that surface is highly folded to increase the area available for gas exchange and gill surface area can indeed scale close to $b=1.0$ if required by metabolic demand (Wegner, 2011; Lefevre et al., 2017, 2018; Wegner and Farrell, 2023). Although gill surface area does generally scale less than $b=1.0$ as predicted by geometric isometry and the GOLT, there are robust datasets showing species-specific scaling of gill surface area close to or even

exceeding $b=1.0$, which would argue against the GOLT (Holeton, 1976; Wegner et al., 2010a; Bigman et al., 2018). Likewise, limited comparisons of the scaling of gill surface area and metabolic rate in the same species has shown that the ratio of gill surface area to metabolic rate does not necessarily decrease with growth (Scheuffele et al., 2021; Somo et al., 2023). However, most of the work to date that examines the links among oxygen, metabolic rate and gill surface area is across species (Gillooly et al., 2016; Bigman et al., 2021, 2023a,b). There are few studies that examine the scaling of gill surface area and metabolic rate for the same species (De Jager and Dekkers, 1975; Gillooly et al., 2016; Bigman et al., 2021), and even fewer studies that estimate gill surface area and metabolic rate in the same individual animals (Li et al., 2018; Luo et al., 2020; Somo et al., 2023). One of the key issues in comparing the allometry of traits, such as gill surface area or metabolic rate, is that the traits are often not measured in individuals of an overlapping body-size range, and when they do overlap, it is often only for a small fraction of the species size range (Bigman et al., 2021; Scheuffele et al., 2021). As a consequence, comparing allometric slope estimates may be confounded by Jensen’s inequality resulting from averaging non-linear (power-law) relationships, particularly of partially non-overlapping size ranges (Denny, 2017; Bigman et al., 2023a,b).

Here, we examined the allometric scaling between oxygen supply (gill surface area) and demand (metabolic rate) using paired estimates of gill surface area with RMR and MMR in 20 California horn shark (*Heterodontus francisci*) individuals over a wide body-size range representing nearly the full ontogeny of the species. This species was chosen because of its ease in laboratory manipulation for determining both RMR and MMR, as well as its inactive, benthic lifestyle, which, according to reviews of fish metabolism, is likely to have a high metabolic allometric slope that could approach $b=1.0$ (Glazier, 2005; Killen et al., 2010). Such a high metabolic allometric slope (and potentially similar allometric slope for gill surface area) would allow for testing predictions of the GOLT. We thus asked four questions. (1) Do the allometric slopes of RMR and MMR differ? (2) If different, is the allometric slope of gill surface area closer to that of RMR or MMR? (3) Is the allometric slope of gill surface area significantly lower than 1.0? (4) Does the ratio of gill surface area to either RMR or MMR decrease with size (ontogeny)? To determine how California horn sharks increase their gill surface area as they grow in size, we also examined the allometric scaling of each gill surface area component (filament length, lamellar frequency and lamellar surface area) and compared each estimate with the values expected under surface-area-to-volume relationships.

MATERIALS AND METHODS

Animal acquisition and husbandry

We used a total of 20 California horn shark [*Heterodontus francisci* (Girard 1855)] individuals ranging in size from 0.039 to 4.44 kg (16.9–89.5 cm total length). We captured 18 individuals between June 2019 and February 2021 as bycatch during overnight gillnet surveys or by hand using SCUBA in Mission Bay in San Diego, CA, USA, and off Scripps Pier in La Jolla, CA, USA. Two of the smallest individuals in our study (0.0387 kg, 0.0590 kg) hatched from eggs laid by an adult female collected at the same time as the other sharks (note: we did not use this adult female in respirometry experiments as gestational and postpartum metabolism was likely to differ from typical resting metabolism). We transported all sharks collected from the wild to the Southwest Fisheries Science Center (SWFSC) Experimental Aquarium in coolers with supplemental oxygen and frequent water changes to maintain oxygen saturation

and reduce waste build-up. We performed all shark capture, transport, husbandry and experimentation according to Institutional Animal Care and Use Committee Protocols of the University of California, San Diego (S00080) and SWFSC (SW1801).

Following collection, we allowed the sharks to acclimate to captivity until they resumed regular feeding for at least 2 weeks before experimentation. We held the sharks at a mean±s.d. temperature of 18.2±0.2°C in 300×150×90 cm oval tanks (length×width×height; ~3200 l) continuously fed with fresh filtered and UV-sterilized seawater (100% air saturation, 33.5‰ salinity). We chose this temperature as it falls at the middle of the natural range and temperature preference for this species (Skelton et al., 2023) and was within approximately 1°C of the ocean temperature at which we collected the individuals. For identification, we took a photograph of the dorsal fin spot pattern on each individual upon arrival. We fed the sharks to satiation every 3 to 5 days using human-grade California market squid (*Doryteuthis opalescens*) and Pacific chub mackerel (*Scomber japonicus*), and we fasted each individual for a minimum of 48 h before experiments to remove the influence of specific dynamic action on metabolic rate estimates (Luongo and Lowe, 2018). We fed the two sharks hatched from eggs and the smallest shark collected from the wild shucked Gould beancalam (*Donax gouldii*) and squid tentacles daily until the sharks were deemed strong enough to be fasted and exercised (10+ weeks post hatch).

Respirometry and experimental setup

We measured oxygen consumption rate (M_{O_2} in mg O₂ h⁻¹) for each individual using respirometers consisting of a holding chamber proportional to the size of the shark and a short recirculation loop containing a fiber optic oxygen sensor and temperature probe connected to either a Fibox 3 or Fibox 4 oxygen meter (Presens, Regensburg, Germany) (Clark et al., 2013; Svendsen et al., 2016; Skelton et al., 2023). We used seven separate respirometer chambers of increasing width and length to accommodate the wide size range of individuals used in this study. The six larger chambers were commercially available acrylic cylinders (Loligo Systems, Denmark) and varied in size, resulting in a total respirometer volume of 5.8 to 52.5 l. The smallest respirometer (2.6 l) was constructed from a 28.1×19.3×7.9 cm rectangular Tupperware outfitted with a recirculating loop like the cylindrical chambers to accommodate the three smallest individuals. The chamber-to-fish volume ratio varied from 11.8:1 to 66.4:1. During trials, we placed the respirometer in a large water bath to maintain a consistent experimental temperature (target 18.0°C, mean 18.2±0.2°C) and to allow the system to be flushed with aerated seawater between oxygen depletion measurements through inlet/outlet one-way check valves on opposing ends of the chamber. Water entering the chamber from both the recirculating loop (constantly flowing) and inlet valve (opened during flush periods) was forced against a splitter or a wide plate to aid in water mixing within the chamber. To reduce bacterial growth, water baths were constantly supplied with fresh, UV-sterilized aerated seawater (salinity 33.5‰, oxygen 100% air saturation) at a rate to fully exchange the bath water every 30–60 min, and we washed the systems with freshwater and detergent or sterilized with ethanol between experiments.

Estimation of resting metabolic rate

We estimated RMR for each individual using automated intermittent flow respirometry (Svendsen et al., 2016; Chabot et al., 2016). One at a time, we moved sharks from their holding tank

to individual respirometer chambers set up within the water bath. Black plastic sheets were draped over the chambers to prevent visual disturbance. When time and space allowed, we ran two individuals at the same time within the water bath, but in individual respirometers separated by a black plastic divider so they could not see each other. Based on preliminary trials, we allowed individuals to acclimate in the respirometer overnight for 12 h to reduce any stress associated with handling and chamber acclimation. We then measured the resting oxygen consumption rate during the first daylight hours of the morning in which sharks were found to be most calm. California horn sharks are nocturnal and relatively inactive, preferring to hide in rock crevices during the day to avoid predators (Meese and Lowe, 2020), and thus showed little to no activity inside the respirometer while at rest.

We used an automated intermittent flow respirometry protocol made up of repeated cycles, each consisting of a closed (10 min) and flush period (5–10 min depending on chamber size). During the closed periods, the automated flush pump turned off and the inflow and outflow check valves sealed the chamber for measurement of oxygen depletion. During the open period, the flush pump turned on to allow fresh, oxygenated seawater to be pumped into the chamber to fully exchange and oxygenate the respirometer water. We began the cycles as soon as we placed the individual within the respirometer chamber and measured oxygen concentration within the recirculating loop once every 5 s.

Within the closed periods, we calculated the M_{O_2} using the equation:

$$M_{O_2} = [(V_r - V_f) \times \beta_{O_2}] / M_f, \quad (1)$$

where V_r is the respirometer chamber volume in liters, V_f is the fish volume (assumed to be equivalent to the fish mass, M_f) and β_{O_2} is the rate of oxygen depletion in the respirometer over time. For each closed period, we removed the first 3 min of oxygen depletion data to allow for any measurement lag associated with water cycling through the system, and then used the following 7 min to estimate M_{O_2} . Following the 12-h acclimation period, we used the mean of the lowest three M_{O_2} measurements occurring during the remaining 5 to 9 h the individual was in the chamber as the RMR estimate for that individual. We measured the background respiration immediately following removal of the individual from the respirometer in RMR pilot experiments when bacteria build-up would have been highest, and found it to be negligible (<3% of resting M_{O_2}) in all but the trial for the smallest individual (body mass 0.0387 kg). For this individual, we calculated the background respiration level during the trial assuming a linear increase over time from just before the individual was placed in the respirometer chamber to just after it was removed (Skelton et al., 2023). We then corrected M_{O_2} for each measurement by subtracting this calculated level of background respiration (Rodgers et al., 2016).

Estimation of maximum metabolic rate

Immediately following estimation of RMR for each shark, we estimated MMR using one of two methods: chase alone or chase with air exposure, hereafter termed ‘chase’ and ‘chase+air’, respectively. Following a 2-day recovery period from the first MMR trial, we used the other MMR method on that individual. We randomly assigned the order of MMR methods for each individual. For both the chase and the chase+air methods, the protocol began by removing the individual from the respirometer chamber following the RMR trial and placing it in a large circular chase tank filled with

aerated seawater siphoned from the holding tank. We then exercised the individual to exhaustion by grabbing and pinching at its tail and by turning it over with gloved hands. We deemed it exhausted once it stopped bursting away and began resting on the bottom of the chase tank between stimuli (usually after 4–7 min of chasing). If undergoing the chase method, we then immediately transferred the individual to the respirometer chamber for measurement of post-exercise oxygen consumption, where we recorded oxygen concentration once every second until the oxygen concentration within the chamber reached 80% saturation (Reidy et al., 1995; Prinzing et al., 2021). Transfer time from the chase tank to the start of oxygen depletion measurements was typically less than 30 s. In the chase+air method, after being chased to exhaustion, we placed the individual in a holding bin without water for 10 min with a wet cloth draped over the eyes and gill slits before transferring it to the respirometer. Owing to their small body size, we separated each MMR trial (chase, chase+air) for the three smallest individuals by at least 4 days to allow the shark to fully recover and feed between trials.

We estimated MMR using a rolling regression model following Prinzing et al. (2021), in which we used the 2-min regression window corresponding to the highest rate of oxygen consumption within the oxygen depletion trace to calculate MMR using Eqn 1. The majority of estimates made with the chase method were higher than those made with the chase+air method, and a linear mixed-effects model with general linear hypothesis test (conducted in R v. 4.2.1, <https://www.r-project.org/>) showed that estimates produced with the MMR chase and MMR chase+air methods did not differ significantly (Table S1, Fig. S1). Thus, only the MMR chase results are shown and used in further analyses below (see Supplementary information for MMR method analysis and MMR chase and chase+air comparison).

Estimation of gill surface area

Following respirometry trials, we euthanized the individual with an overdose of the anesthetic MS-222 for estimation of total gill surface area. We patted the shark dry for mass measurement, following which we removed the head posterior to the last gill arch and fixed it in seawater-buffered 10% formalin for a minimum of 2 weeks for tissue fixation before beginning gill dissections.

We estimated gill surface area for each shark as:

$$A = L_{\text{fil}} \times 2n_{\text{lam}} \times A_{\text{lam}}, \quad (2)$$

where L_{fil} is the total length of all gill filaments on both sides of the head, n_{lam} is the lamellar frequency (i.e. the mean number of lamellae per unit length on one side of a filament, multiplied by two to account for lamellae on both sides of the filament), and A_{lam} is the mean bilateral surface area of a lamella (Wegner, 2011, 2016). To determine these dimensions, we removed all five gill arches from the right side of the head and counted all filaments on all nine hemibranchs. We divided each hemibranch evenly into eight bins of filaments. We took a magnified photo of the median filament in each bin, which we assumed to be representative of all filaments in that bin (Meiji Techno America EMZ-8TR microscope with Moticam 5+ camera, San Jose, CA, USA). We measured the length of this filament, including the section beneath the gill arch branchial canopy (Wegner et al., 2010b; Wegner, 2016), using ImageJ imaging software (National Institutes of Health, Bethesda, MD, USA, Java 1.8.0_172). We calculated the total length of all filaments on all hemibranchs on the right side of the head by multiplying the length of the median filament in each bin by the

total number of filaments in that bin, then summing the length of all filaments in all bins. We then doubled this length to account for the length of filaments on the left side of the head, which were not measured.

Following filament measurements, we removed the median filament from each bin for lamellar measurements. We turned each excised filament on its side to show the lamellae and took a magnified photo at the base, middle and tip sections for estimation of lamellar frequency (number of lamellae per mm) using ImageJ software. We then made a cross section at each of these three locations on the filament to take magnified photographs of the extended lamellae on both sides of the filament. We estimated lamellar surface area in mm^2 using ImageJ software by tracing the outline of a lamella on one side of the filament, then doubling it to calculate the bilateral surface area of the lamella. We estimated mean lamellar frequency (mm^{-1}) by averaging lamellar frequency measurements taken at each of the base, middle and tip of each median filament, multiplying this mean by the total length of all filaments in that bin to give the total number of lamellae per bin, summing the total number of lamellae in all bins, then dividing this by the total length of all filaments. We estimated average lamellar surface area (mm^2) by taking the mean of lamellar surface area measurements taken at the same three locations as lamellar frequency on each filament, multiplying this mean by the total number of lamellae in that bin to give a total lamellar area per bin, summing the total lamellar area for all bins, then dividing by the total number of lamellae. We measured lamellar frequency and surface area on all median filaments from all nine hemibranchs on one side of the head on the first dissected individual. These measurements showed that the posterior hemibranch on the second gill arch was most representative of the gills as a whole, and thus for subsequent sharks, we based lamellar frequency and mean lamellar surface area measurements solely on this hemibranch (Wegner, 2011).

Statistical analysis

We conducted all data processing and analyses in R version 4.2.1 (<https://www.r-project.org/>).

We estimated the allometric scaling coefficients of RMR ($\text{mg O}_2 \text{ h}^{-1}$), MMR ($\text{mg O}_2 \text{ h}^{-1}$), aerobic scope ($\text{mg O}_2 \text{ h}^{-1}$) and gill surface area (cm^2) as a function of body mass (kg) using ordinary least squares (OLS) regression. We \log_{10} -transformed the data prior to fitting the model [see White and Kearney (2011) and Bigman et al. (2018) for discussion on fitting power laws with linear regression (our approach) versus nonlinear regression]. We then checked the residuals for normality and homoscedasticity. The gill surface area and body mass relationship appeared to have a breakpoint. We fit a broken stick regression with \log_{10} total gill surface area as a function of \log_{10} body mass using the segmented function from the package segmented (version 1.6-0, <https://CRAN.R-project.org/package=segmented>), and used AIC to compare this model with the equivalent OLS model.

We tested for a difference between the allometric slopes of RMR and MMR by fitting a linear mixed-effects model, where the \log_{10} metabolic rate estimate was a function of \log_{10} body mass with metabolic rate type as an interaction term and individual as a random effect. We then used the emmeans function from the package emmeans to compare allometric slope estimates from our linear mixed-effects model (version 1.8.1-1, <https://CRAN.R-project.org/package=emmeans>). This analysis is similar to an ANCOVA but accounts for the influence of the random effect of individual in our model.

Using just the 17 largest shark individuals, we examined the ratio of gill surface area to metabolic rate, calculated as total gill surface area (cm^2) divided by either RMR or MMR ($\text{mg O}_2 \text{ h}^{-1}$) for each individual and then \log_{10} transformed (Scheuffele et al., 2021). We excluded the three smallest individuals from this analysis as their gill surface areas appeared to deviate from that of the larger sharks as seen through an inflection point at the fourth smallest shark (see Results). We then estimated the allometric slope of the ratio estimates for each of \log_{10} gill surface area to resting metabolic rate (GSA/RMR) and \log_{10} GSA/MMR against \log_{10} body mass.

Finally, we examined the allometric slopes of each gill surface area component to understand how California horn sharks increase gill surface area as they grow. We examined the scaling of each gill surface area component including \log_{10} total filament length (cm), \log_{10} average lamellar frequency (mm^{-1}) and \log_{10} mean bilateral lamellar surface area (mm^2) as a function of \log_{10} body mass, using OLS regression. Similar to gill surface area, there appeared to be an inflection point in the relationship between \log_{10} lamellar surface area and \log_{10} body mass, and we also fit a broken stick regression to these data and compared this with the equivalent OLS models using AIC (version 1.6-0, <https://CRAN.R-project.org/package=segmented>).

RESULTS

The allometric slope of MMR was greater than 1.0 ($b=1.073\pm 0.040$, $\pm 95\%$ CI) and similar to, but significantly steeper than, the allometric slope of RMR ($b=0.966\pm 0.058$; Table 1, Fig. 1A). The higher allometric slope for MMR in relation to RMR led to an allometric slope greater than 1.0 for absolute aerobic scope ($b=1.098\pm 0.022$; Table 1, Fig. 1B). When the allometric scaling of gill surface area was examined using a broken stick regression, this model estimated an inflection point at the fourth smallest individual (0.203 kg body mass) and produced slope estimates of $b=0.564\pm 0.261$ for individuals smaller than 0.203 kg and $b=1.012\pm 0.113$ for individuals larger than 0.203 kg (Table 1, Fig. 1C). When modeled across the full sample size of California horn shark using OLS regression, the allometric slope of gill surface area was $b=0.877\pm 0.067$ (Table 1, Fig. 1C). Comparing these models using AIC revealed that the broken stick regression model was a better fit to the gill surface area data relative to the OLS regression (Table 1).

When we examined the allometric slope of the ratio of gill surface area (cm^2) to metabolic rate ($\text{mg O}_2 \text{ h}^{-1}$) for the 17 largest individuals, we found that the amount of gill surface area per unit RMR remained effectively constant ($b=0.040\pm 0.188$), whereas the amount of gill surface area per unit MMR decreased slightly but not significantly (the 95% confidence interval crossed zero; $b=-0.102\pm 0.122$; Fig. 2).

The allometric slopes for the gill components of total filament length (cm), average lamellar frequency (mm^{-1}) and mean bilateral lamellar surface area (mm^2) were $b=0.400\pm 0.017$ ($\pm 95\%$ CI), $b=-0.103\pm 0.011$ and $b=0.577\pm 0.073$, respectively (Fig. 3). However, for lamellar surface area, a broken stick regression was deemed a better fit than the OLS regression model based on AIC scores (Table 1), and this model estimated an inflection point at the fourth smallest individual, with an allometric slope estimate of $b=0.196\pm 0.257$ for sharks less than 0.203 kg and $b=0.742\pm 0.111$ for individuals larger than 0.203 kg.

DISCUSSION

Our results suggest that the scaling of oxygen supply and demand, as measured by gill surface area and metabolic rate, are closely matched in the California horn shark. When viewed across a nearly complete body size range, the allometric slope of RMR was $b=0.966$ and that of MMR was significantly greater at $b=1.073$; as such, aerobic scope increased with body mass ($b=1.098$). Surprisingly, we found that the relationship between gill surface area and body mass was best explained by a broken stick regression model in which small sharks showed a shallower allometric slope, whereas the gill surface area of larger individuals scaled at $b=1.012$, in between that of RMR and MMR. The findings that gill surface area scales near $b=1.0$ and that neither the ratio of GSA/RMR nor GSA/MMR shows a significant negative relationship are inconsistent with predictions of the GOLT and suggest that aerobic metabolism is not limited by gill surface area in this species. In the following, we first discuss the allometric scaling of metabolic rate and compare the slope of RMR with that of MMR. Second, we compare the scaling of metabolic rate with that of gill surface area and then discuss how our findings fit into the larger framework of metabolic scaling in the context of oxygen supply and demand. Finally, we discuss the potential physiological underpinnings of the allometric scaling of gill surface area.

Table 1. Model parameter estimates of linear and segmented relationships between body mass (\log_{10} kg) and resting (RMR) and maximum (MMR) metabolic rate (\log_{10} $\text{mg O}_2 \text{ h}^{-1}$), absolute aerobic scope (\log_{10} $\text{mg O}_2 \text{ h}^{-1}$) and gill surface area (GSA, \log_{10} cm^2) at a mean temperature of 18.2°C in the California horn shark, *Heterodontus francisci*, using ordinary least squares (OLS) and broken stick (BS) regression

Trait	Model	Adjusted r^2	a (\pm s.e.)	b (\pm s.e.)	b 95% CI	AIC
RMR	OLS	0.985	1.626 \pm 0.018	0.966 \pm 0.028	\pm 0.058	
MMR	OLS	0.994	2.369 \pm 0.012	1.073 \pm 0.019	\pm 0.040	
Aerobic scope	OLS	0.992	2.280 \pm 0.014	1.098 \pm 0.022	\pm 0.046	
GSA (cm^2)	BS	0.985	3.344 $^{>0.203 \text{ kg}}$ 3.034 $^{<0.203 \text{ kg}}$	1.012 \pm 0.053 $^{>0.203 \text{ kg}}$ 0.564 \pm 0.123 $^{<0.203 \text{ kg}}$	\pm 0.113 \pm 0.261	-43.7
	OLS	0.976	3.377 \pm 0.02	0.877 \pm 0.032	\pm 0.067	-35.4
GSA/RMR ratio	OLS	-0.052	1.719 \pm 0.036	0.040 \pm 0.088	\pm 0.188	
GSA/MMR ratio	OLS	0.12	0.985 \pm 0.024	-0.102 \pm 0.057	\pm 0.122	
Total filament length (cm)	OLS	0.992	4.053 \pm 0.005	0.400 \pm 0.008	\pm 0.017	
Mean lamellar frequency (mm^{-1})	OLS	0.950	0.972 \pm 0.003	-0.103 \pm 0.005	\pm 0.011	
Mean bilateral lamellar surface area (mm^2)	BS	0.968	0.013 $^{>0.203 \text{ kg}}$ -0.365 $^{<0.203 \text{ kg}}$	0.742 \pm 0.052 $^{>0.203 \text{ kg}}$ 0.196 \pm 0.121 $^{<0.203 \text{ kg}}$	\pm 0.111 \pm 0.257	-44.3
	OLS	0.935	0.053 \pm 0.022	0.577 \pm 0.035	\pm 0.073	-31.7

Allometric regression parameters for the equation $\log_{10} Y = a + b \log_{10} M$, where a is the scaling coefficient or intercept, b is the allometric slope, M is mass (kg) and Y is the trait. 95% confidence intervals are given where available. The superscripts ' $>0.203 \text{ kg}$ ' and ' $<0.203 \text{ kg}$ ' indicate estimates for each size range, respectively. For both gill surface area and lamellar area, AIC indicated that the BS regression model was a better fit relative to the OLS regression model. Ratio analyses were conducted excluding the three smallest sharks (see Materials and Methods).

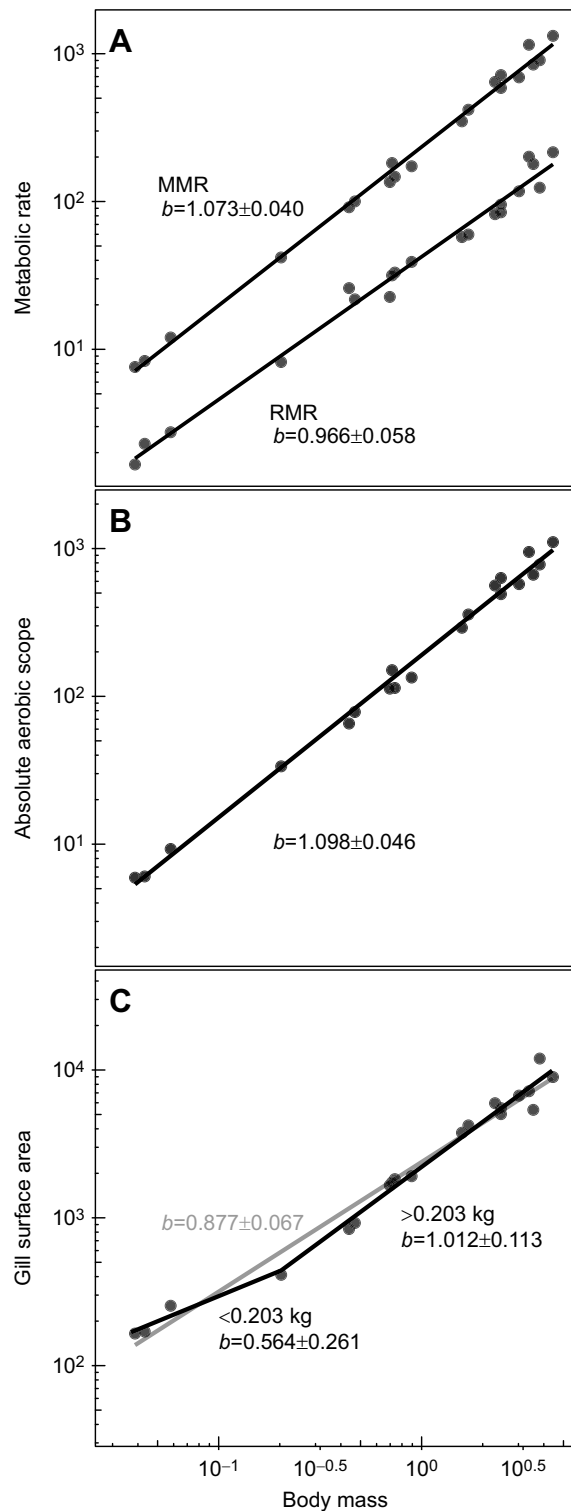


Fig. 1. Allometric scaling of resting metabolic rate (RMR), maximum metabolic rate (MMR), absolute aerobic scope and gill surface area (GSA) in the California horn shark, *Heterodontus francisci*, as a function of body mass on a \log_{10} - \log_{10} scale. (A) RMR and MMR (both $\text{mg O}_2 \text{ h}^{-1}$), (B) absolute aerobic scope ($\text{mg O}_2 \text{ h}^{-1}$) and (C) GSA (cm^2). Metabolic data were determined at $18.2 \pm 0.2^\circ\text{C}$ (mean \pm s.d.). The relationship of GSA with body mass (C) is shown using both the better-fit broken stick regression (solid black line) compared with the ordinary least squares regression (gray line). Allometric slopes are shown for each regression segment (see Table 1 for other regression parameters).

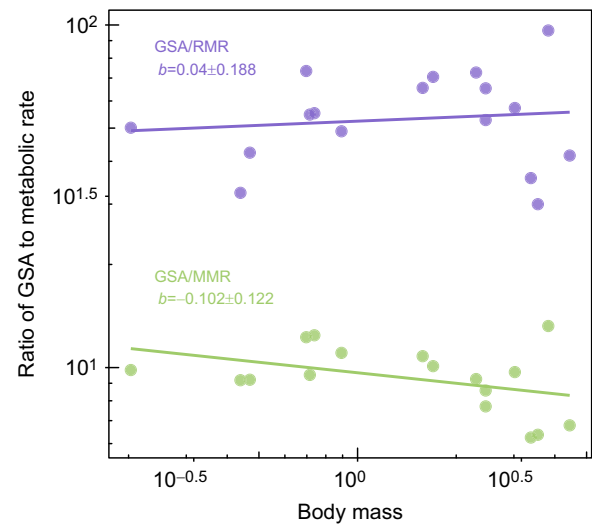


Fig. 2. The allometric relationship of the ratio of GSA (cm^2) to RMR (purple, $\text{mg O}_2 \text{ h}^{-1}$) and MMR (green, $\text{mg O}_2 \text{ h}^{-1}$) on a \log_{10} - \log_{10} scale for the 17 largest California horn sharks examined in the present study. Slope and 95% confidence interval values are noted for each regression. Each point represents the amount of gill surface area an individual possesses relative to oxygen consumption ($\text{cm}^2/\text{mg O}_2 \text{ h}^{-1}$) at that individual's body mass at 18.2°C .

Across a body size range representing the near-complete ontogeny of the California horn shark, our results showed that the mean allometric slopes of RMR and MMR were around $b=1.0$. This pattern is consistent with the metabolic level boundaries hypothesis, which predicts that relatively inactive species are less likely to be influenced by surface area limits on fluxes of resources and wastes, and thus can have metabolic rate slopes nearer to 1.0, whereas more active species may be more constrained by surface-area-to-volume ratios and generally exhibit relatively shallower metabolic allometric slopes (Glazier, 2005; Killen et al., 2010). Killen et al. (2010) showed that this activity-scaling pattern holds across 89 fish species binned into one of four ecological lifestyle categories (pelagic, benthopelagic, benthic and bathyal) or four swimming modes (thunniform, carangiform, subcarangiform and anguilliform), and suggested that these factors may be partly responsible for the variation in allometric slope estimates observed across species.

The metabolic level boundaries hypothesis also predicts that the slope of MMR will generally scale steeper than the slope of RMR as metabolic rate during strenuous exercise should be influenced primarily by the volume-related scaling of muscle power, yielding an allometric slope nearer to 1.0, whereas lower, relatively sustainable metabolic rates should be more closely tied to surface-area-to-volume ratios and scale with a shallower allometric slope (Glazier, 2005, 2009). Although the allometric slope of MMR in the California horn shark is significantly greater than that of RMR, the slope of RMR is already close to $b=1.0$. This suggests that other factors are likely at play, with the diverging slopes of RMR and MMR indicating an increase in aerobic scope as this species grows. This appears consistent with ontogenetic changes seen in the behavior of the California horn shark in which juvenile sharks appear to prefer relatively shallow and sandy habitats, where they make limited movements and likely feed on soft-bodied and inactive invertebrate prey, whereas adults occupy and navigate more complex rocky reefs and are known to travel up to 13 km in a single night of more active foraging (Compagno, 2002; Kolmann

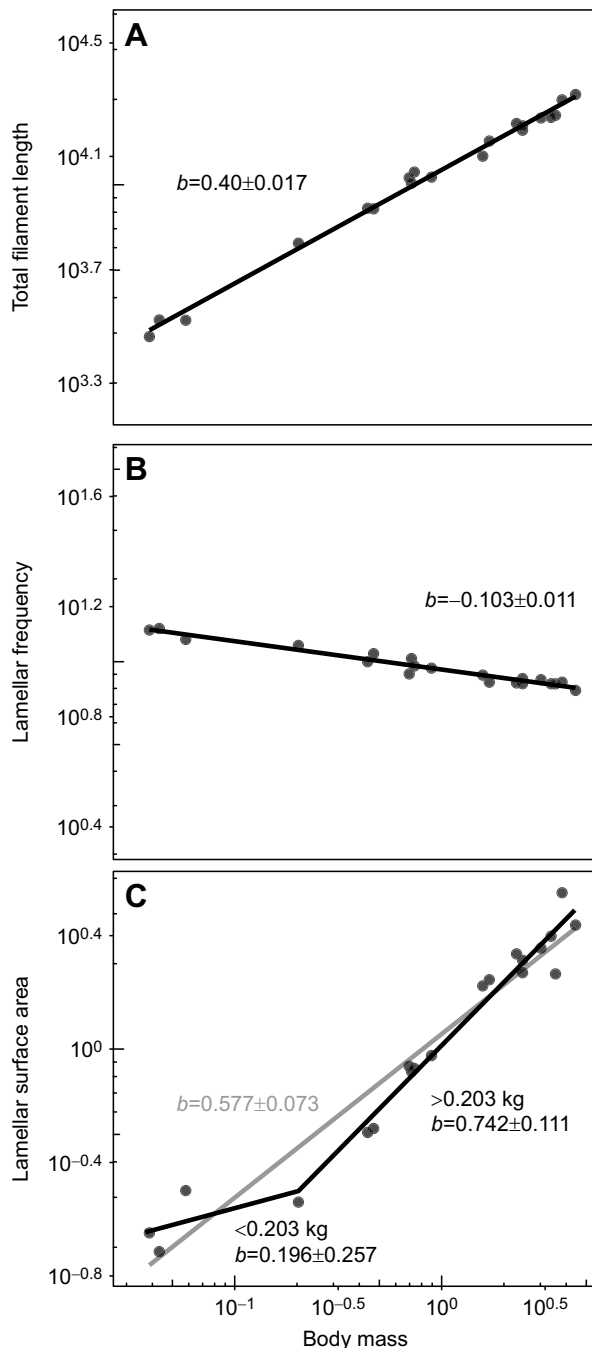


Fig. 3. The relationship between gill surface area components and body mass (kg) for 20 California horn shark individuals. (A) Total filament length (cm), (B) average lamellar frequency (mm^{-1}) and (C) mean bilateral lamellar surface area (mm^2). The relationship between lamellar surface area and body mass (C) is shown using both the better-fit broken stick regression (solid black line) compared with the ordinary least squares regression (gray line). Allometric slopes are shown for each regression segment (see Table 1 for other regression parameters).

and Huber, 2009; Cortés-Fuentes et al., 2020; Meese and Lowe, 2020). Although numerous species show steeper allometric slopes for MMR than RMR, there are examples where this is not the case. In fishes of the family Cyprinidae (Actinopterygii: Cypriniformes), an opposite pattern has been found in which the allometric slope of RMR is steeper than or similar to that of MMR (Zhang et al., 2014; Luo et al., 2015), which the authors conclude may be related to the

low relative contribution of muscular energy expenditure to whole-body metabolism in these inactive species. Thus, more paired measures of RMR and MMR across ontogeny in species from a wider range of activity levels are needed to help us better understand the interplay of oxygen uptake, oxygen demand and activity level.

In contrast to the scaling of metabolic rate, we found that the scaling of gill surface area in the California horn shark was best estimated by a broken stick regression model, indicating a shift in gill growth and demand with ontogeny. The inflection point in the gill surface area–body mass relationship shows a steepening of the allometric slope near 30 cm total length, corresponding to the size at which California horn sharks are thought to begin transitioning from their juvenile to adolescent life stage (35 cm) (Ebert et al., 2013). This inflection point is not seen in either the MMR or RMR regressions, and suggests a potential disconnect between oxygen supply and demand prior to the inflection point, at which point gill surface area appears to begin to track metabolism. Unlike most teleosts, oviparous elasmobranchs such as the California horn shark emerge from their egg cases resembling adults, covered in calcareous dermal denticles, and mainly respire across their gill tissue (Toulmond et al., 1982; Rodda and Seymour, 2008). Thus, at least at later stages of embryonic development within the egg case, they must rely on their gills as the sole gas exchange surface, possibly resulting in a relatively large gill surface area as an adaptation to protect against potential hypoxia in their surrounding environment or within the potentially diffusion-limited egg case itself (Di Santo et al., 2016). Further, embryonic metabolic rates may be relatively high in oviparous elasmobranchs because of the need for highly active tail beating to ventilate the egg capsule and circulate water (Leonard et al., 1999). It appears that California horn sharks (and likely other oviparous elasmobranchs) may require a larger gill surface area as developing embryos than immediately post hatch. Thus, once hatched, California horn sharks appear to possess excess gill surface area relative to their oxygen demand, resulting in a lower gill surface area allometric slope during early life until faster gill growth is again needed to meet metabolic needs, at which point gill surface area scales similarly to metabolic rate with an allometric slope falling between that of RMR and MMR. This broken stick pattern in the allometry of gill surface area in juvenile California horn sharks contrasts with the initially very steep scaling of gill surface area in larval teleost fishes that reflects rapid teleost gill development following initial reliance on cutaneous gas exchange during early larval stages (Oikawa and Itazawa, 1985; Rombough and Moroz, 1997). Future work should test whether our findings for the California horn shark apply across other oviparous elasmobranchs.

Comparison of the allometric slope of gill surface area with that of RMR and MMR can provide potential insight into factors influencing rates of oxygen uptake and demand and activity. Previous work has suggested that the allometric slope of gill surface area should fall closer to that of MMR in order to supply the fish with sufficient oxygen for activity above rest (Hughes, 1972, 1984). This makes sense when we consider that the allometric slope of MMR is often steeper than that of RMR and that fish require sufficient gill surface area to meet maximum aerobic energy requirements (Hughes, 1984; Bishop, 1999; Killen et al., 2007). However, California horn sharks do not seem to follow this pattern, as their gill surface area ($b=1.012$) appears to scale in between that of RMR ($b=0.966$) and MMR ($b=1.073$). This may be related to their general inactivity. For example, tagging and tracking studies of California horn sharks showed that they spend most (88.1–93.3%) of the day at rest in shelters and only actively forage for

approximately 50% of the night, while mostly feeding on sessile or inactive prey (Meese and Lowe, 2020). Likewise, horn sharks have relatively few predators and use camouflage and their dorsal spines to deter predators rather than utilizing an active flee response. Thus, California horn sharks may not often require the gill surface area necessary for relatively high levels of energy expenditure, and hence their gill area may not need to scale similar to MMR. This appears consistent with recent work on less-active teleost species, in which gill surface area scales in between that of MMR and RMR (Somo et al., 2023) or even closer to that of RMR (Luo et al., 2020). Additional paired data of gill surface area and metabolic rate may help determine whether such trends hold across larger samples of active and inactive species. However, in a comparison across 12 elasmobranch species, Bigman et al. (2018) did not find any trends in the allometric slope of gill surface area related to maximum size, habitat type, or caudal fin aspect ratio (a measure of activity level). This highlights the need for further work on additional species that vary in activity level and habitat use.

In addition to providing insight into California horn shark activity and life history, our results argue against suppositions made by the GOLT that posit that geometric constraints of gill surface area limit fish metabolism (Pauly, 2010, 2021; Pauly and Cheung, 2017). Specifically, our results show that gill surface area scales at $b=1.012$ in the California horn shark after the inflection point (0.203 kg), which differs from the GOLT argument that gill surface area must scale less than $b=1.0$ owing to two-dimensional surface area constraints. Likewise, our results show that gill surface area in the California horn shark scales similar to the allometric slopes of both RMR and MMR, and thus the scaling of both the GSA/RMR and GSA/MMR ratios do not differ significantly from zero. If either ratio showed a negative relationship, it could indicate a potential mismatch in oxygen supply and demand (Scheuffele et al., 2021). In contrast, our data suggest there is not a mismatch in the allometric scaling of oxygen supply and demand in the California horn shark, and these results closely match recent work on the tidepool sculpin (*Oligocottus maculosus*), an inactive teleost species (Somo et al., 2023). Finally, an increase in aerobic scope ($b=1.098$) and the high allometric slope of MMR ($b=1.073$) over the entire ontogeny of California horn shark examined here shows that the capacity for aerobic performance (and hence oxygen consumption) actually disproportionately increases with growth, suggesting that oxygen uptake at the gills cannot be limiting, as suggested by the GOLT (which would predict a decline in aerobic scope with increasing body size; Pauly, 2010, 2021). These findings are consistent with widely held physiological views that the gills are adapted to match metabolic needs, rather than metabolism being constrained by gill surface area (Wegner, 2011; Lefevre et al., 2017, 2018). Thus, the relatively low oxygen demands of this generally inactive species appear amply met by its available gill surface area.

Examination of individual gill components, specifically filament length, lamellar frequency and lamellar surface area, provides insight into how gill surface area in the California horn shark scales at $b\sim 1.0$. Based on geometric isometry (i.e. equal gill growth in all dimensions), gill surface area would theoretically scale at $b=2/3$ or 0.67 (i.e. a two-dimensional surface area divided by a three-dimensional volume or mass) (Wegner, 2011). When broken down into individual dimensions, filament length should thus theoretically scale at $b=0.33$ (length/volume), lamellar frequency at $b=-0.33$ (length⁻¹/volume) and lamellar surface area at $b=0.67$ (surface area/volume), which when summed (0.33–0.33+0.67) result in a total of gill surface area allometric slope of $b=0.67$ (Wegner, 2011, 2016; Wegner and Farrell, 2023). However, in most

fishes, although filament length and lamellar surface area generally scale similarly to these geometric predictions, lamellar frequency generally scales much higher than geometric isometry would predict because the thickness of the lamellae and spacing in between adjacent lamellae do not greatly increase with growth. This allows the allometric slope of lamellar frequency to approach $b=0$ instead of $b=-0.33$, and thus gill surface area typically scales higher than the predicted $b=0.67$ (Palzenberger and Pohla, 1992; Wegner et al., 2010a; Wegner, 2011; Wegner and Farrell, 2023). We found that the California horn shark achieves a high gill surface area allometric slope by minimizing changes to lamellar frequency ($b=-0.103$) as in other fishes, but also by disproportionately increasing filament length ($b=0.400$) and lamellar surface area ($b=0.742$ in sharks greater than 0.203 kg), resulting in a total gill surface area allometric slope of $b\sim 1.0$. The disproportionately high scaling of filament length and lamellar surface area could necessitate a concomitant increase in the volume of the parabranchial chambers as an individual grows. Although there are no measures of ontogenetic scaling in the head or parabranchial chamber sizes for the California horn shark, the closely related Pork Jackson shark (*Heterodontus portusjacksoni*) shows a disproportionate increase in head length and width in proportion to total body length as the shark matures (Powter et al., 2010). This may offer an increase in space in the branchial cavities available for gills, reducing any possible morphological constraint to gill surface area that might be more of an issue for more active shark species in which cranial streamlining would be more important (Wootton et al., 2015). Although filament length and lamellar frequency scale similarly across the entire ontogeny of California horn shark, lamellar surface area scaling is most accurately described with a broken stick model with an inflection point at the same location as gill surface area (0.203 kg). Thus, the growth of gill lamellae appears slow upon hatching and to subsequently shift to faster growth to align gill surface area with metabolic demand at larger sizes. Such changes in lamellar size mirror those seen in fishes exposed to hypoxia or increased temperature in which a greater gill surface area is needed when the dissolved oxygen content of the water is low or metabolic demands are elevated (Sollid and Nilsson, 2006; Chapman, 2007; Wegner and Farrell, 2023). Thus, lamellar surface area seems to be a highly plastic component of gill surface area that can be rapidly manipulated to meet changing oxygen demands across fish groups.

In summary, our findings constitute a thorough look at the allometric scaling patterns of RMR, MMR, aerobic scope and gill surface area using paired estimates within the same individuals. This allows for more precise exploration of the relationship between metabolic rate and gill surface area by removing complications arising from comparing multiple data sets with contrasting body masses and species (Gillooly et al., 2016; Scheuffele et al., 2021; Bigman et al., 2021). Taken together, our results show that for some species, such as the relatively inactive California horn shark, the allometric slope of metabolic rate and gill surface area can approach or even exceed $b=1.0$. The unusually steep allometric slopes found here emphasize the need for more work examining these traits in species of varying activity levels and across ecological lifestyles. Finally, the inflection point found in the allometric scaling of gill surface area in the California horn shark highlights the importance of examining a species' complete body-size range in allometric studies and the potential importance of life-stage-dependent influences on allometric slopes.

Acknowledgements

The authors thank Kathy Swiney, Garrett Seibert, Stephanie Fan and Dr Joshua Lonthair for help in care and husbandry of the sharks used in this study in the

SWFSC Experimental Aquarium, as well as Dr Joshua Lonthair, Dr Tony Williams and the Dulvy lab at Simon Fraser University for feedback on this research. Results and Discussion of this paper were reproduced or modified from the MSc thesis of Tanya Prinzing (Simon Fraser University, 2021).

Competing interests

The authors declare no competing or financial interests.

Author contributions

Conceptualization: T.S.P., J.S.B., N.K.D., N.C.W.; Methodology: T.S.P., J.S.B., Z.R.S., N.K.D., N.C.W.; Validation: T.S.P., Z.R.S.; Formal analysis: T.S.P.; Investigation: T.S.P., Z.R.S., N.C.W.; Resources: N.K.D., N.C.W.; Data curation: T.S.P., J.S.B.; Writing - original draft: T.S.P.; Writing - review & editing: J.S.B., Z.R.S., N.K.D., N.C.W.; Visualization: T.S.P.; Supervision: N.K.D., N.C.W.; Project administration: N.K.D., N.C.W.; Funding acquisition: N.K.D., N.C.W.

Funding

This study was funded by the Natural Science and Engineering Research Council of Canada (NSERC), the Canada Research Chairs Program and the United States National Marine Fisheries Service. Open Access funding provided by University of California, San Diego. Deposited in PMC for immediate release.

Data availability

All data and code are available at <https://github.com/tanya-prinzing/HS-MS-Ranalysis>.

References

- Auer, S. K., Killen, S. S. and Rezende, E. L. (2017). Resting vs. active: a meta-analysis of the intra- and inter-specific associations between minimum, sustained, and maximum metabolic rates in vertebrates. *Funct. Ecol.* **31**, 1728-1738. doi:10.1111/1365-2435.12879
- Bigman, J. S., Pardo, S. A., Prinzing, T. S., Dando, M., Wegner, N. C. and Dulvy, N. K. (2018). Ecological lifestyles and the scaling of shark gill surface area. *J. Morphol.* **279**, 1716-1724. doi:10.1002/jmor.20879
- Bigman, J. S., M'Gonigle, L. K., Wegner, N. C. and Dulvy, N. K. (2021). Respiratory capacity is twice as important as temperature in explaining patterns of metabolic rate across the vertebrate tree of life. *Sci. Adv.* **7**, eabe5163. doi:10.1126/sciadv.abe5163
- Bigman, J. S., Wegner, N. C. and Dulvy, N. K. (2023a). Revisiting a central prediction of the gill oxygen limitation theory: gill area index and growth performance. *Fish. Fish.* **24**, 354-366. doi:10.1111/faf.12730
- Bigman, J. S., Wegner, N. C. and Dulvy, N. K. (2023b). Gills, growth and activity across fishes. *Fish. Fish.* doi:10.1111/faf.12757
- Bishop, C. M. (1999). The maximum oxygen consumption and aerobic scope of birds and mammals: getting to the heart of the matter. *Proc. R. Soc. B* **266**, 2275-2281. doi:10.1098/rspb.1999.0919
- Brett, J. R. and Glass, N. R. (1973). Metabolic rates and critical swimming speeds of sockeye salmon (*Oncorhynchus nerka*) in relation to size and temperature. *J. Fish. Res. Board Canada* **30**, 379-387. doi:10.1139/f73-068
- Brown, J. H., Gillooly, J. F., Allen, A. P., Savage, J. M. and West, G. B. (2004). Toward a metabolic theory of ecology. *Ecology* **85**, 1771-1789. doi:10.1890/03-9000
- Chabot, D., Steffensen, J. F. and Farrell, A. P. (2016). The determination of standard metabolic rate in fishes. *J. Fish. Biol.* **88**, 81-121. doi:10.1111/jfb.12845
- Chapman, L. J. (2007). Morpho-physiological divergence across aquatic oxygen gradients in fishes. In *Fish Respiration and Environment* (ed. M. N. Fernandes, F. T. Rantin, M. L. Glass and B. G. Kapoor), pp. 13-39. Enfield, New Hampshire: Science Publishers.
- Cheung, W. W. L., Sarmiento, J. L., Dunne, J., Frölicher, T. L., Lam, V. W. Y., Palomares, M. L. D., Watson, R. and Pauly, D. (2013). Shrinking of fishes exacerbates impacts of global ocean changes on marine ecosystems. *Nat. Clim. Chang.* **3**, 254-258. doi:10.1038/nclimate1691
- Clarke, T. M., Wabnitz, C. C., Striegel, S., Frölicher, T. L., Reygondeau, G. and Cheung, W. W. (2021). Aerobic growth index (AGI): An index to understand the impacts of ocean warming and deoxygenation on global marine fisheries resources. *Prog. Oceanogr.* **195**, 102588. doi:10.1016/j.pocan.2021.102588
- Clark, T. D., Sandblom, E. and Jutfelt, F. (2013). Aerobic scope measurements of fishes in an era of climate change: respirometry, relevance and recommendations. *J. Exp. Biol.* **216**, 2771-2782. doi:10.1242/jeb.084251
- Compagno, L. J. V. (2002). *Sharks of the World. An Annotated and Illustrated Catalogue of Shark Species Known to Date: Bullhead, mackerel and carpet sharks (Heterodontiformes, Lamniformes and Orectolobiformes)*. FAO Species Catalogue for Fishery Purposes, Vol. 2. Rome: FAO.
- Cortés-Fuentes, C., Simental-Angiano, M. R., Galván-Magaña, F. and Medina-López, M. A. (2020). Feeding habits of the horn shark *Heterodontus francisci* (Girard, 1855) in the northwest of Baja California Sur, Mexico. *J. Appl. Ichthyol.* **36**, 197-202. doi:10.1111/jai.14004
- De Jager, S. and Dekkers, W. (1975). Relations between gill structure and activity in fish. *Netherlands J. Zool.* **25**, 276-308. doi:10.1163/002829675X00290
- Denny, M. (2017). The fallacy of the average: on the ubiquity, utility and continuing novelty of Jensen's inequality. *J. Exp. Biol.* **220**, 139-146. doi:10.1242/jeb.140368
- Deutsch, C., Penn, J. L. and Seibel, B. (2020). Metabolic trait diversity shapes marine biogeography. *Nature* **585**, 557-562. doi:10.1038/s41586-020-2721-y
- Deutsch, C., Ferrel, A., Seibel, B., Pörtner, H.-O. and Huey, R. B. (2015). Climate change tightens a metabolic constraint on marine habitats. *Science* **348**, 1132-1136. doi:10.1126/science.aaa1605
- Di Santo, V., Tran, A. H. and Svendsen, J. C. (2016). Progressive hypoxia decouples activity and aerobic performance of skate embryos. *Conserv. Physiol.* **4**, cov067. doi:10.1093/conphys/cov067
- Ebert, D. A., Fowler, S. and Compagno, L. (2013). *Sharks of the World: A Fully Illustrated Guide*. Plymouth, MA: Wild Nature Press.
- Gillooly, J. F., Gomez, J. P., Mavrodiev, E. V., Rong, Y. and McLaMORE, E. S. (2016). Body mass scaling of passive oxygen diffusion in endotherms and ectotherms. *Proc. Natl. Acad. Sci. USA* **113**, 5340-5345. doi:10.1073/pnas.1519617113
- Glazier, D. S. (2005). Beyond the '3/4-power law': variation in the intra- and interspecific scaling of metabolic rate in animals. *Biol. Rev.* **80**, 611-662. doi:10.1017/S1464793105006834
- Glazier, D. S. (2009). Activity affects intraspecific body-size scaling of metabolic rate in ectothermic animals. *J. Comp. Physiol. B* **179**, 821-828. doi:10.1007/s00360-009-0363-3
- Glazier, D. S. (2010). A unifying explanation for diverse metabolic scaling in animals and plants. *Biol. Rev.* **85**, 111-138. doi:10.1111/j.1469-185X.2009.00095.x
- Graham, J. B. and Laurs, R. M. (1982). Metabolic rate of the albacore tuna *Thunnus alalunga*. *Mar. Biol.* **72**, 1-6. doi:10.1007/BF00393941
- Holeton, G. F. (1976). Respiratory morphometrics of white and red blooded Antarctic fish. *Comp. Biochem. Physiol.* **54A**, 215-220. doi:10.1016/S0300-9629(76)80100-4
- Hughes, G. M. (1972). Morphometrics of fish gills. *Respir. Physiol.* **14**, 1-25. doi:10.1016/0034-5687(72)90014-X
- Hughes, G. M. (1984). Scaling of respiratory areas in relation to oxygen consumption of vertebrates. *Experientia* **40**, 519-524. doi:10.1007/BF01982313
- Jerde, C. L., Kraskura, K., Eliason, E. J., Csik, S. R., Stier, A. C. and Taper, M. L. (2019). Strong evidence for an intraspecific metabolic scaling coefficient near 0.89 in fish. *Front. Physiol.* **10**, 1-17. doi:10.3389/fphys.2019.01166
- Killen, S. S., Costa, I., Brown, J. A. and Gampert, A. K. (2007). Little left in the tank: Metabolic scaling in marine teleosts and its implications for aerobic scope. *Proc. R. Soc. B Biol. Sci.* **274**, 431-438. doi:10.1098/rspb.2006.3741
- Killen, S. S., Atkinson, D. and Glazier, D. S. (2010). The intraspecific scaling of metabolic rate with body mass in fishes depends on lifestyle and temperature. *Ecol. Lett.* **13**, 184-193. doi:10.1111/j.1461-0248.2009.01415.x
- Killen, S. S., Glazier, D. S., Rezende, E. L., Clark, T. D., Atkinson, D., Willener, A. S. T. and Halsey, L. G. (2016). Ecological influences and morphological correlates of resting and maximal metabolic rates across teleost fish species. *Am. Nat.* **187**, 592-606. doi:10.1086/685893
- Kolmann, M. A. and Huber, D. R. (2009). Scaling of feeding biomechanics in the horn shark *Heterodontus francisci*: ontogenetic constraints on durophagy. *Zoology* **112**, 351-361. doi:10.1016/j.zool.2008.11.002
- Lefevre, S., Mckenzie, D. J. and Nilsson, G. E. (2017). Models projecting the fate of fish populations under climate change need to be based on valid physiological mechanisms. *Glob. Chang. Biol.* **23**, 3449-3459. doi:10.1111/gcb.13652
- Lefevre, S., Mckenzie, D. J. and Nilsson, G. E. (2018). In modelling effects of global warming, invalid assumptions lead to unrealistic projections. *Glob. Chang. Biol.* **24**, 553-556. doi:10.1111/gcb.13978
- Lefevre, S., Wang, T. and McKenzie, D. J. (2021). The role of mechanistic physiology in investigating impacts of global warming on fishes. *J. Exp. Biol.* **224**, jeb238840. doi:10.1242/jeb.238840
- Leonard, J. B. K., Summers, A. P. and Koob, T. J. (1999). Metabolic rate of embryonic little skate, *Raja erinacea* (Chondrichthyes: Batoidea): the cost of active pumping. *J. Exp. Zool.* **283**, 13-18. doi:10.1002/(SICI)1097-010X(1999101)283:1<13::AID-JEZ3>3.0.CO;2-S
- Li, G., Lv, X., Zhou, J., Shen, C., Xia, D., Xie, H. and Luo, Y. (2018). Are the surface areas of the gills and body involved with changing metabolic scaling with temperature? *J. Exp. Biol.* **221**, jeb174474. doi:10.1242/jeb.174474
- Luo, Y., He, D., Li, G., Xie, H., Zhang, Y. and Huang, Q. (2015). Intraspecific metabolic scaling exponent depends on red blood cell size in fishes. *J. Exp. Biol.* **218**, 1496-1503. doi:10.1242/jeb.117739
- Luo, Y., Li, Q., Zhu, X., Zhou, J., Shen, C., Xia, D., Djiba, P. K., Xie, H., Lv, X., Jia, J. et al. (2020). Ventilation frequency reveals the roles of exchange surface areas in metabolic scaling. *Physiol. Biochem. Zool.* **93**, 13-22. doi:10.1086/706115
- Luongo, S. M. and Lowe, C. G. (2018). Seasonally acclimated metabolic Q₁₀ of the California horn shark, *Heterodontus francisci*. *J. Exp. Mar. Biol. Ecol.* **503**, 129-135. doi:10.1016/j.jembe.2018.02.006
- Meese, E. N. and Lowe, C. G. (2020). Active acoustic telemetry tracking and tri-axial accelerometers reveal fine-scale movement strategies of a non-obligate ram ventilator. *Mov. Ecol.* **8**, 1-17. doi:10.1186/s40462-020-0191-3

- Muir, B. S. and Hughes, G. M. (1969). Gill dimensions for three species of tunny. *J. Exp. Biol.* **51**, 271-285.
- Nilsson, G. E. and Östlund-Nilsson, S. (2008). Does size matter for hypoxia tolerance in fish? *Biol. Rev.* **83**, 173-189. doi:10.1111/j.1469-185X.2008.00038.x
- Norin, T. and Gamperl, A. K. (2017). Metabolic scaling of individuals vs. populations: evidence for variation in scaling exponents at different hierarchical levels. *Funct. Ecol.* **32**, 379-388. doi:10.1111/1365-2435.12996
- Oikawa, S. and Itazawa, Y. (1985). Gill and body surface areas of the carp in relation to body mass, with special reference to the metabolism-size relationship. *J. Exp. Biol.* **117**, 1-14. doi:10.1242/jeb.117.1.1
- Palzenberger, M. and Pohla, H. (1992). Gill surface area of water-breathing freshwater fish. *Rev. Fish Biol. Fish.* **2**, 187-216.
- Pauly, D. (2010). Gasping fish and panting squids: oxygen, temperature and the growth of water-breathing animals. International Ecology Institute, Oldendorf/Luhe, Germany.
- Pauly, D. (2021). The gill-oxygen limitation theory (GOLT) and its critics. *Sci. Adv.* **7**, eabc6050. doi:10.1126/sciadv.abc6050
- Pauly, D. and Cheung, W. W. L. (2017). Sound physiological knowledge and principles in modeling shrinking of fishes under climate change. *Glob. Chang. Biol.* **24**, e15-e26. doi:10.1111/gcb.13831
- Pörtner, H. O. and Knust, R. (2007). Climate change affects marine fishes through the oxygen limitation of thermal tolerance. *Science* **315**, 95-97. doi:10.1126/science.1135471
- Pörtner, H. O. and Farrell, A. P. (2008). Physiology and climate change. *Science* **322**, 690-692. doi:10.1126/science.1163156
- Powter, D. M., Gladstone, W. and Platell, M. (2010). The influence of sex and maturity on the diet, mouth morphology and dentition of the Port Jackson shark, *Heterodontus portusjacksoni*. *Mar. Freshw. Res.* **61**, 74-85. doi:10.1071/MF09021
- Prinzing, T. S., Zhang, Y., Wegner, N. C. and Dulvy, N. K. (2021). Analytical methods matter too: Establishing a framework for estimating maximum metabolic rate for fishes. *Ecol. Evol.* **11**, 9987-10003. doi:10.1002/ece3.7732
- Reidy, S. P., Nelson, J. A., Tang, Y. and Kerr, S. R. (1995). Post-exercise metabolic rate in Atlantic cod and its dependence on the method of exhaustion. *J. Fish. Biol.* **47**, 377-386. doi:10.1111/j.1095-8649.1995.tb01907.x
- Rodda, K. R. and Seymour, R. S. (2008). Functional morphology of embryonic development in the Port Jackson shark *Heterodontus portusjacksoni* (Meyer). *J. Fish. Biol.* **72**, 961-984. doi:10.1111/j.1095-8649.2007.01777.x
- Rodgers, G. G., Tenzing, P. and Clark, T. D. (2016). Experimental methods in aquatic respirometry: the importance of mixing devices and accounting for background respiration. *J. Fish. Biol.* **88**, 65-80. doi:10.1111/jfb.12848
- Rombough, P. J. and Moroz, B. M. (1997). The scaling and potential importance of cutaneous and branchial surfaces in respiratory gas exchange in larval and juvenile walleye *Stizostedion vitreum*. *J. Exp. Biol.* **200**, 2459-2468. doi:10.1242/jeb.200.18.2459
- Rubalcaba, J. G., Verberk, W. C. E. P., Hendriks, A. J., Saris, B. and Woods, H. A. (2020). Oxygen limitation may affect the temperature and size dependence of metabolism in aquatic ectotherms. *Proc. Natl. Acad. Sci. USA* **117**, 31963-31968. doi:10.1073/pnas.2003292117
- Scheuffele, H., Jutfelt, F. and Clark, T. D. (2021). Investigating the gill-oxygen limitation hypothesis in fishes: intraspecific scaling relationships of metabolic rate and gill surface area. *Conserv. Physiol.* **9**, coab040. doi:10.1093/conphys/coab040
- Sibly, R. M., Brown, J. H. and Kodric-Brown, A. (2012). *Metabolic Ecology: A Scaling Approach*. Oxford: Wiley-Blackwell.
- Skelton, Z. R., Prinzing, T. S., Hastings, P. A. and Wegner, N. C. (2023). Laboratory-based measures of temperature preference and metabolic thermal sensitivity provide insight into habitat utilization of juvenile California horn shark (*Heterodontus francisci*) and leopard shark (*Triakis semifasciata*). *J. Fish. Biol.* **102**, 829-843. doi:10.1111/jfb.15307
- Sollid, J. and Nilsson, G. E. (2006). Plasticity of respiratory structures – adaptive remodeling of fish gills induced by ambient oxygen and temperature. *Respir. Physiol. Neurobiol.* **154**, 241-251. doi:10.1016/j.resp.2006.02.006
- Somo, D. A., Chu, K. and Richards, J. G. (2023). Gill surface area allometry does not constrain the body mass scaling of maximum oxygen uptake rate in the tidepool sculpin, *Oligocottus maculosus*. *J. Comp. Physiol. B.* **193**, 425-438. doi:10.1007/s00360-023-01490-9
- Svendsen, M. B. S., Bushnell, P. G. and Steffensen, J. F. (2016). Design and setup of intermittent-flow respirometry system for aquatic organisms. *J. Fish. Biol.* **88**, 26-50. doi:10.1111/jfb.12797
- Toulmond, A., Dejours, P. and Truchot, J. P. (1982). Cutaneous O₂ and CO₂ exchanges in the dogfish, *Scyliorhinus canicula*. *Respir. Physiol.* **48**, 169-181. doi:10.1016/0034-5687(82)90078-0
- Wegner, N. C. (2011). Gill respiratory morphometrics. In *Encyclopedia of Fish Physiology: From Genome to Environment* (ed. A. P. Farrell), pp. 803-811. San Diego, CA: Academic Press.
- Wegner, N. C. (2016). Elasmobranch gill structure. In *Physiology of Elasmobranch Fishes: Structure and Interaction with Environment* (ed. R. E. Shadwick, A. P. Farrell and C. J. Brauner), pp. 101-151. New York: Academic Press.
- Wegner, N. C. and Farrell, A. P. (2023). Plasticity in gill morphology and function. In *Encyclopedia of Fish Physiology*, 2nd edn (ed. S. L. Alderman and T. Gillis). Academic Press. doi:10.1016/B978-0-323-90801-6.00028-8
- Wegner, N. C., Sepulveda, C. A., Bull, K. B. and Graham, J. B. (2010a). Gill morphometrics in relation to gas transfer and ram ventilation in high-energy demand teleosts: scombrids and billfishes. *J. Morphol.* **271**, 36-49. doi:10.1002/jmor.10777
- Wegner, N. C., Sepulveda, C. A., Olson, K. R., Hyndman, K. A. and Graham, J. B. (2010b). Functional morphology of the gills of the shortfin mako, *Isurus oxyrinchus*, a lamnid shark. *J. Morphol.* **271**, 937-948. doi:10.1002/jmor.10845
- White, C. R. and Kearney, M. R. (2011). Metabolic scaling in animals: methods, empirical results, and theoretical explanations. *Compr. Physiol.* **4**, 231-256. doi:10.1002/cphy.c110049
- White, C. R., Phillips, N. F. and Seymour, R. S. (2006). The scaling and temperature dependence of vertebrate metabolism. *Biol. Lett.* **2**, 125-127. doi:10.1098/rsbl.2005.0378
- White, C. R., Alton, L. A., Bywater, C. L., Lombardi, E. J. and Marshall, D. J. (2022). Metabolic scaling is the product of life-history optimization. *Science* **377**, 834-839. doi:10.1126/science.abm7649
- Wootton, T. P., Sepulveda, C. A. and Wegner, N. C. (2015). Gill morphometrics of the thresher sharks (Genus *Alopias*): Correlation of gill dimensions with aerobic demand and environmental oxygen. *J. Morphol.* **276**, 589-600. doi:10.1002/jmor.20369
- Zhang, Y., Huang, Q., Liu, S., He, D., Wei, G. and Luo, Y. (2014). Intraspecific mass scaling of metabolic rates in grass carp (*Ctenopharyngodon idellus*). *J. Comp. Physiol. B* **184**, 347-354. doi:10.1007/s00360-014-0802-7